Numerical Modeling of an Integrated Vehicle Fluids System Loop for Pressurizing a Cryogenic Tank

by

A.C. LeClair, A. Hedayat and A. K. Majumdar
Propulsion System Department
NASA/Marshall Space Flight Center
Huntsville, Alabama - 35812

Abstract

This paper presents a numerical model of the pressurization loop of the Integrated Vehicle Fluids (IVF) system using the Generalized Fluid System Simulation Program (GFSSP). The IVF propulsion system, being developed by United Launch Alliance to reduce system weight and enhance reliability, uses boiloff propellants to drive thrusters for the reaction control system as well as to run internal combustion engines to develop power and drive compressors to pressurize propellant tanks. NASA Marshall Space Flight Center (MSFC) conducted tests to verify the functioning of the IVF system using a flight-like tank. GFSSP, a finite volume based flow network analysis software developed at MSFC, has been used to support the test program. This paper presents the simulation of three different test series, comparison of numerical prediction and test data and a novel method of presenting data in a dimensionless form. The paper also presents a methodology of implementing a compressor map in a system level code.

Nomenclature

A	=	area
ETA	=	compressor efficiency
g_c , J	=	conversion constant
$\bar{m}$	=	non-dimensional mass flowrate
$\dot{m}$	=	mass flowrate
N	=	compressor speed (RPM)
$\bar{p}$	=	non-dimensional pressure
p	=	pressure
P_{ul}	=	ullage pressure
Q	=	volumetric flowrate
R	=	gas constant
r	=	radius
$\bar{T}$	=	non-dimensional temperature
T	=	Temperature
T_{ul}	=	ullage temperature
U	=	velocity
ρ	=	density
γ	=	specific heat ratio
Δh	=	enthalpy rise across compressor
Δp	=	pressure rise across compressor

I. Introduction

For the past several years, United Launch Alliance (ULA) has been developing a propulsion system called Integrated Vehicle Fluids (IVF) [1] to improve the functional and reliability limits of upper stages for long duration space missions. The intent of IVF is to replace the helium storage system and hypergolic thrusters in order to reduce system weight and enhance reliability. IVF uses boil-off propellants to drive thrusters for the reaction control system as well as to run a small Internal Combustion Engine (ICE). The produced thrust is used for maneuvering the vehicle and to settle propellants aft during coast flight. The ICE produces shaft power that is converted into electrical power for charging avionics batteries and driving hydrogen and oxygen compressors. The vented boil-off propellants are heated in heat exchangers that use the warm coolant of the ICE as the hot fluid. Then, the propellant tanks are pressurized with the heated gases leaving the heat exchangers.

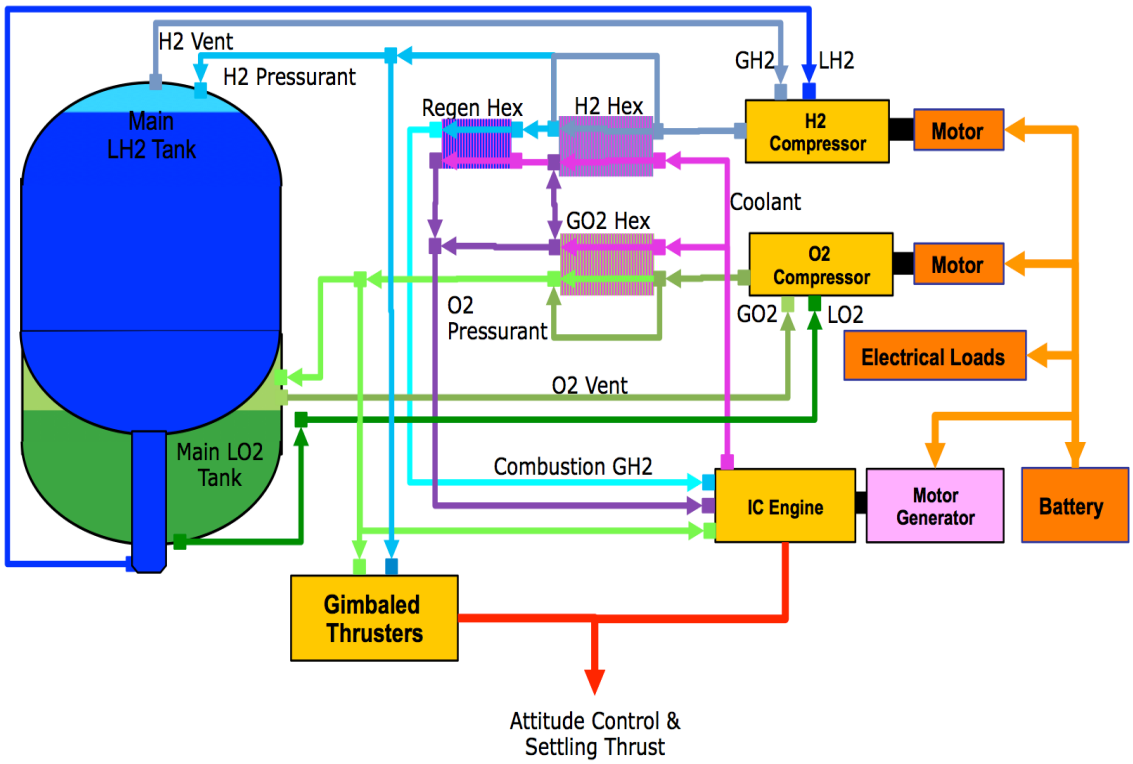

Figure 1. Simplified Schematic of IVF System [1]

Figure 1 shows a simplified schematic of a proposed IVF system. The pressurization system of the tank consists of a fluid loop with a compressor and heat exchanger instead of a helium tank in a conventional propulsion system. The compressor intakes propellant vapor from the tank ullage and drives it through a heat exchanger to heat it before sending the vapor back to the tank for pressurization. The heat exchanger receives heat from the coolant of the Internal Combustion Engine (ICE) which runs using the boil-off

from liquid hydrogen and oxygen tank. The ICE provides power to the compressor and battery. Zegler [1] provides more details of the entire system.

NASA Space Technology Mission Directorate's Evolvable Cryogenics Project has tested the IVF system at Marshall Space Flight Center (MSFC). The test program has been conducted in several phases. In phase A, a flight-like tank has been tested to measure boil-off and pressurization at various levels using both liquid hydrogen (LH2) and nitrogen (LN2). Phase B testing included a pressurization loop consisting of a blower and heat exchanger. In phase B testing, the compressor was not available and substituted with a blower, and the ICE coolant was heated by an electric heater. In phase C, the compressor replaced the blower and the coolant was heated by the exhaust heat of the ICE which ran with the facility supply of hydrogen and oxygen. Prior to the Phase C test, the compressor was characterized by a Max Flow Test.

An efficient and robust system level numerical model is essential to design and optimize the test program to meet all objectives of the test program. The MSFC-developed Generalized Fluid System Simulation Program (GFSSP) has been used to develop a numerical model of the IVF loop for different phases of the test program. The other purpose is to develop a validated numerical model of the IVF system that can be used to assess the feasibility of using IVF system for the Exploration Upper Stage (EUS) of the Space Launch System (SLS).

In an earlier modeling paper [2], a multi-node model of ullage space for computing pressurization and boil-off and an integrated numerical model of tank, IVF Loop and Heat Exchanger was presented. A reasonable agreement with Phase-A test data was obtained for both boil-off and pressurization. In the integrated model, a unique method was developed to combine a system (Tank and IVF loop) and component (heat exchanger); two models exchange data during the iterative cycle until interface boundary conditions are converged.

One of the objectives for phase B testing was to investigate the performance of an injector assembly to supply pressurant into the tank to promote mixing between entering hot gas and resident cold gas in the ullage. There were two types of injectors used in the test: Quad and single tube. The intent was to reduce the temperature of the gas leaving through the vent line to IVF loop. Therefore, in phase B, in order to capture turbulence mixing, a CFD code was used to model the thermo-fluid dynamics of the ullage, while the system-level code GFSSP was used to model the IVF loop and Heat Exchanger. The main purpose of this paper is to describe the modeling of Phase B Test and the modeling technique of compressor characteristics in GFSSP.

II. Mathematical Formulation & Computer Program

GFSSP is a finite volume-based network flow analysis program for analyzing thermo-fluid systems. A fluid network consists of boundary nodes, internal nodes, and branches to represent a fluid system. Boundary and internal nodes are connected through branches in series or parallel arrangements. At boundary nodes, pressures and temperatures are

specified. Mass and energy conservation equations are solved in internal nodes. Flowrates are calculated in branches. A thermal system consists of solid and ambient nodes connected with conductors. A fluid and solid node are connected with a solid to fluid conductor to model conjugate heat transfer.

The mathematical closure is described in Table 1. GFSSP uses a pressure-based scheme as pressure is computed from the mass conservation equation. The mass and momentum conservation equations and thermodynamic equation of state are solved simultaneously by the Newton-Raphson method while the energy conservation equations of fluid and solid are solved separately but are implicitly coupled with the other equations stated above. The conservation equations are solved in conjunction with the thermodynamic equation of state. From the computed pressure and enthalpy at the nodes, all other thermodynamic properties including density, viscosity, and thermal conductivity are evaluated from built-in thermodynamic property programs. For the saturated condition, vapor quality is calculated from liquid and vapor enthalpies at the node pressure. Density and other thermo-physical properties of the liquid-vapor mixture are calculated as a function of vapor quality. Further details of the mathematical formulation and solution procedure are described in reference [3].

Table 1. Mathematical closure.

Unknown Variables	Available Equations to Solve
Pressure	Mass conservation equation
Flowrate	Momentum conservation equation
Fluid temperature	Energy conservation equation of fluid
Solid temperature	Energy conservation equation of solid
Fluid mass (unsteady flow)	Thermodynamic equation of state

Figure 2 describes the three major parts of the GFSSP structure. The first part is the Graphical User Interface, VTASC (Visual Thermo-fluid Analyzer of Systems and Components). VTASC allows users to create a flow circuit by a point-and-click paradigm, and creates the GFSSP input file after the completion of the model building process. It can also create a customized GFSSP executable by compiling and linking User Subroutines with the Solver Module of the code. Users can run GFSSP from VTASC and post-process the results in the same environment. The second major part of the program is the Solver and Property Module. This is the heart of the program that reads the input data file and generates the required conservation equations for all internal nodes and branches with the help of thermodynamic property data. It also interfaces with User Subroutines to receive any specific inputs from users. Finally, it creates output files for VTASC to read and display results. The User Subroutine is the third major part of the program, consisting of several blank subroutines that are called by the Solver Module. These subroutines allow the users to incorporate any new physical model, resistance option, fluid, etc., in the model.

Figure 3 shows the schematic of the mathematical closure and inter-dependence of the variables that requires an iterative scheme to solve the system of equations shown in Table – 1.

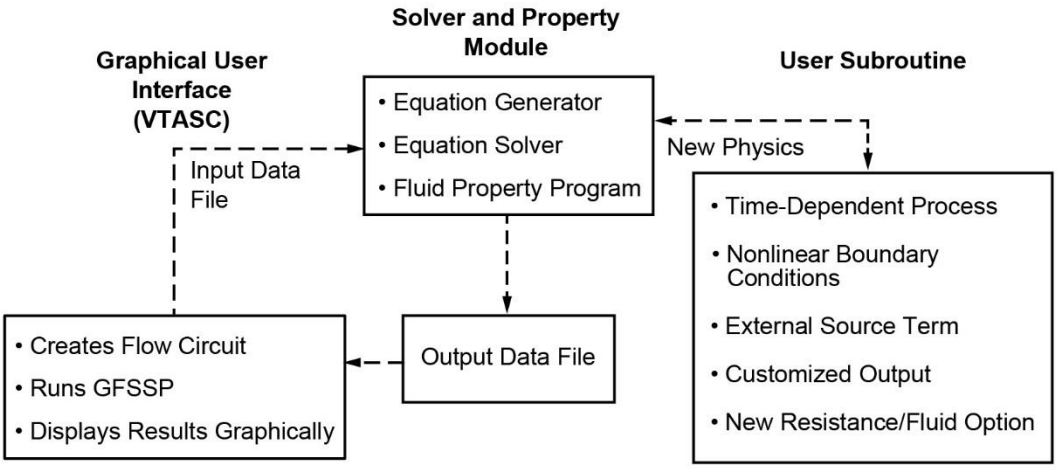

Figure 2. GFSSP's structure showing the interaction of three major modules.

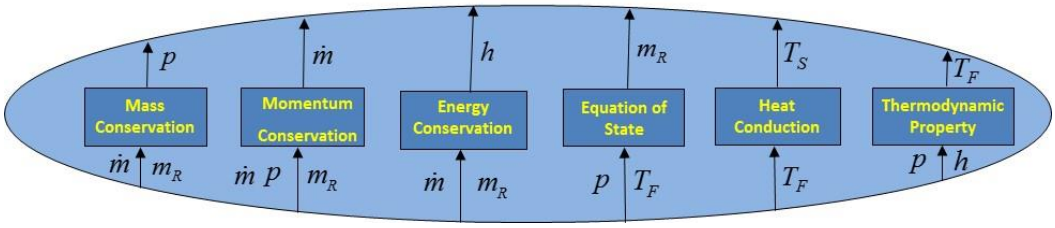

Figure 3. Schematic showing the mathematical closure and inter-relation of the variables

III. **Test Program**

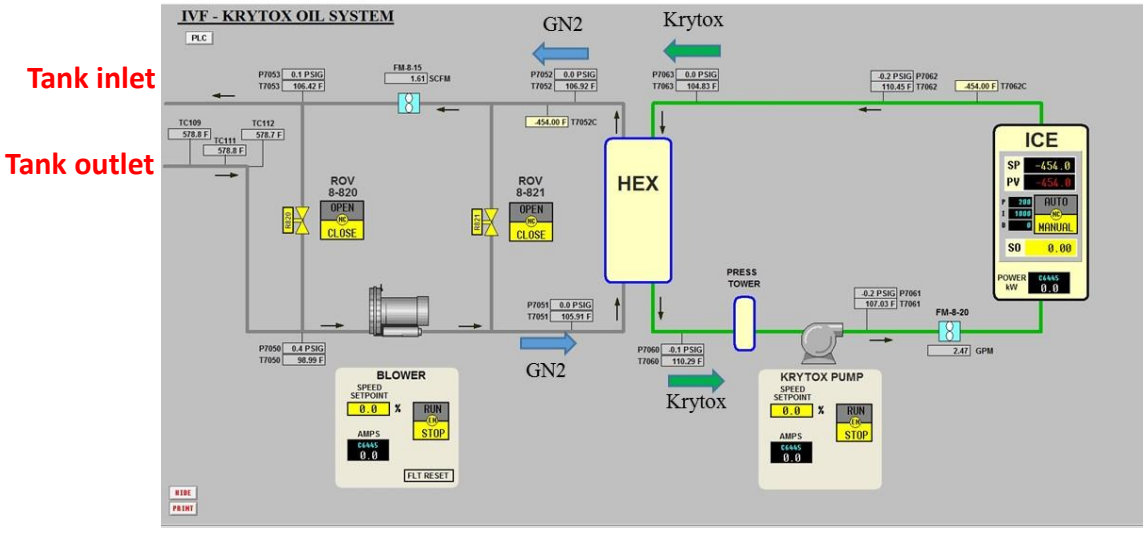

Figure 4. Phase B Test Schematic

The Phase B Test Schematic of the IVF Loop is shown in Figure 4. Nitrogen gas, drawn from the tank by the blower, travels through the Heat Exchanger (HEX) to pick up heat from ICE coolant Krytox and return to the tank to pressurize the ullage. There were three series of tests called Astros, Braves and Cubs. In the Astros series, the tank was pressurized with facility pressurant using a quad injector. It had an open loop with vent gas exit to the ambient. In the Braves series, no facility pressurant was used. The tank was pressurized with a closed loop. However, the flow bypassed the Heat Exchanger. In the Cubs series, closed loop pressurization was used with the Heat Exchanger bypass closed. In all three test series, the fill level in the tank was 75%.

Figure 5. IVF Loop tested at MSFC

Figure 5 shows the IVF loop with Blower, Heat Exchanger and Bypass line in the East Test Area at MSFC.

Prior to Phase C testing the Max Flow Test was conducted to quantify the performance of the ULA/IVF compressor/heat exchanger assembly. Figure 6 shows the schematic of the Max Flow Test. A compressor map was developed from this test which was later incorporated in GFSSP to model the compressor in the IVF loop for a flight vehicle.

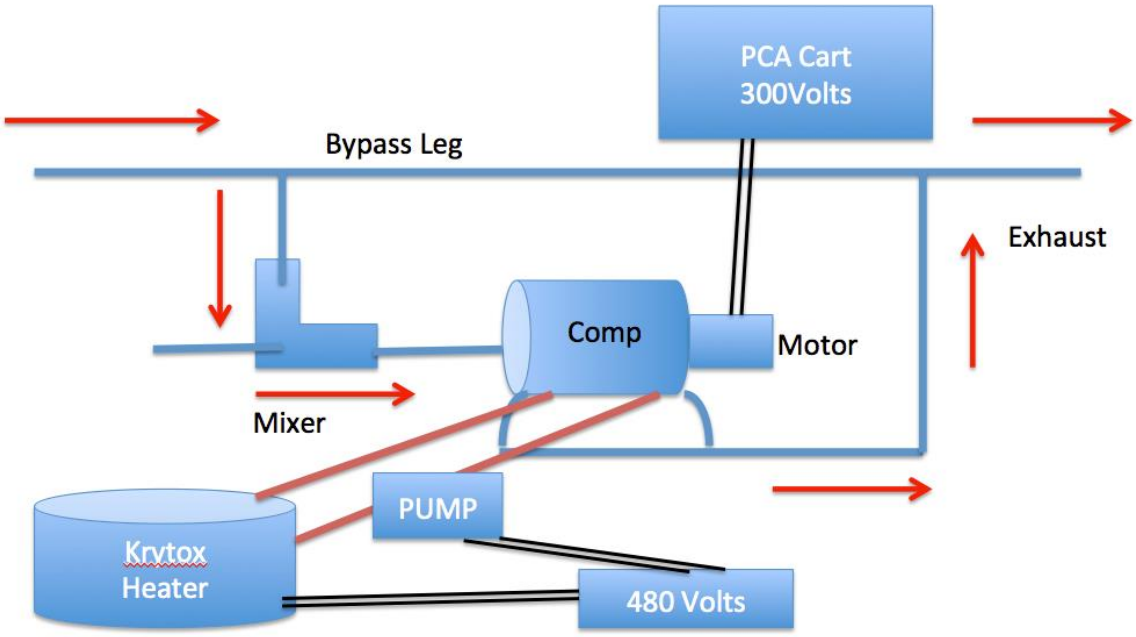

Figure 6. A Schematic of the Max Flow Bench. (Blue and red lines indicate wetted fluid lines, and the black lines denote power to components)

IV. GFSSP Models and Discussion of Results

This section describes GFSSP models and results of Heat Exchanger, Astros, Braves and Cubs series of experiments and the modeling technique of introducing compressor map in GFSSP. The results are expressed in non-dimensional form. Pressures and temperatures are normalized with inlet dynamic head and flowrates are normalized with maximum flowrate that can occur in the vent pipe when the flow is choked.

Dimensionless pressure: $\bar{p} = \frac{p g_c}{\rho_{inlet} U_{inlet}^2}$

Dimensionless temperature: $\bar{T} = \frac{RT g_c}{U_{inlet}^2}$

Dimensionless flowrate: $\overline{m} = \frac{\dot{m}}{\dot{m}_{max}}$

where $\dot{m}_{max} = A_{vent} P_{ul} \sqrt{\frac{g_c \gamma}{RT_{ul}} \left(\frac{2}{\gamma+1}\right)^{\gamma+1/\gamma-1}}$

A. Heat Exchanger Model

A counter-flow heat exchanger has been used to extract heat from Krytox which is a coolant for the ICE. GN2 is heated by Krytox. Figure 7 shows the Heat Exchanger cross-section and the GFSSP model is shown in Figure 8. The Dittus-Boelter equation has been used to compute heat transfer coefficient between solid and fluid nodes.

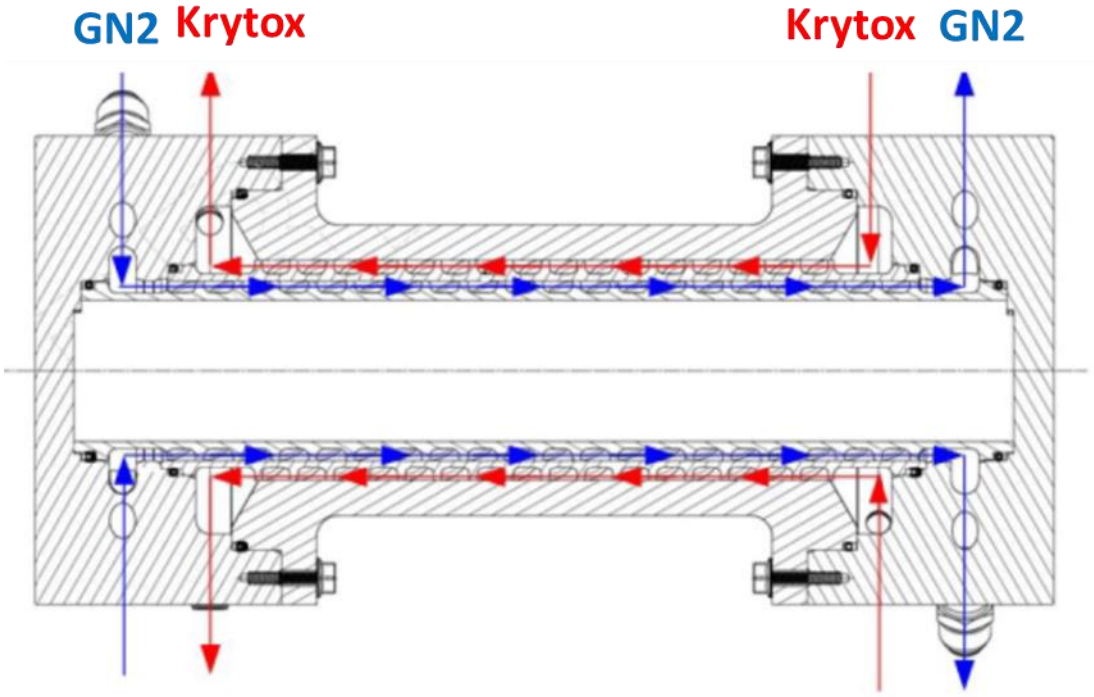

Figure 7. Cross-sectional view of Heat Exchanger

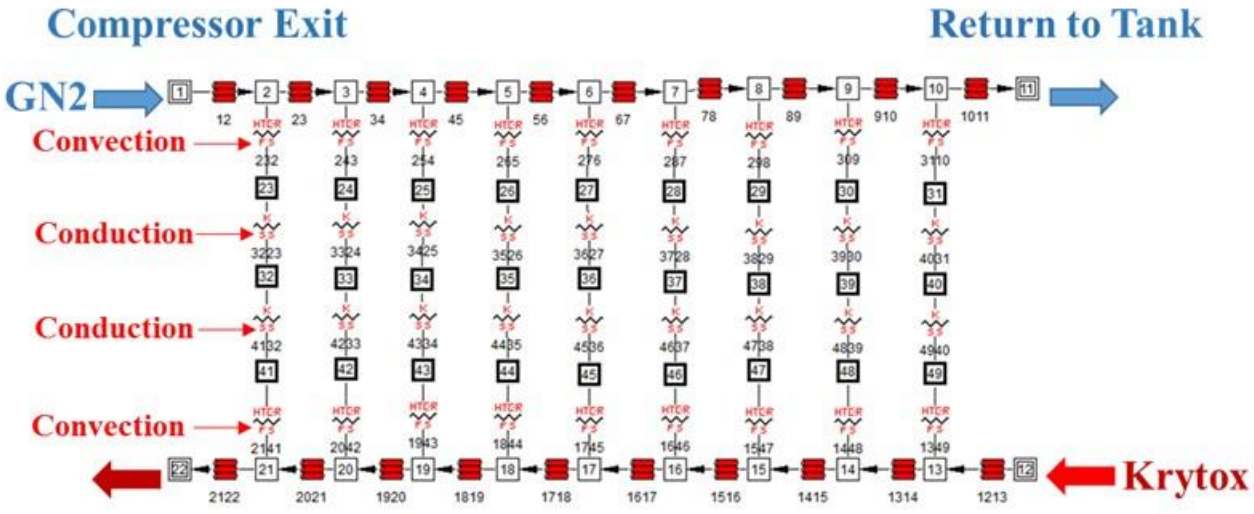

Figure 8. GFSSP model of Heat Exchanger

The comparison between GFSSP predictions and test data is shown in Table - 2

Table 2. Comparison of HEX outlet temperature between model and test data

Case No.	Inlet Temperature	Outlet Temperature Test	Outlet Temperature GFSSP	Discrepancy
	$\bar{T}_{inlet}$	$\bar{T}_{outlet}$	$\bar{T}_{outlet}$	%
1	1.94E+01	2.46E+01	2.49E+01	1.16
2	2.64E+01	2.98E+01	3.12E+01	4.74
3	1.20E+01	1.45E+01	1.49E+01	2.57
4	9.39E+01	1.13E+02	1.16E+02	2.37
5	2.72E+01	3.04E+01	3.18E+01	4.39
6	8.15E+01	1.02E+02	1.00E+02	-1.61
7	2.41E+01	2.85E+01	2.89E+01	1.27
8	1.95E+01	2.11E+01	2.19E+01	3.72
9	9.50E+01	1.03E+02	1.05E+02	1.16
10	2.95E+01	3.18E+01	3.23E+01	1.57
11	2.19E+01	2.29E+01	2.35E+01	2.43

The discrepancy between model and test data is less than 5%, which can be attributed to uncertainties in measurement and heat transfer coefficient correlation.

B. Astros Model

In the Astros test series, facility pressurant was used to pressurize the tank and the IVF loop was open with vent gas exiting to ambient. Modeling was performed in cases where the Variable Position Valve (VPV) was opened in steps and the Blower Motor was held at 100% power. Separate steady-state models were developed for the VPV and blower to characterize the resistance coefficient and blower efficiency to match measured pressure difference and flowrate characteristics. With the calibrated resistance coefficient and blower efficiency, the unsteady loop model was developed and shown in Figure 9.

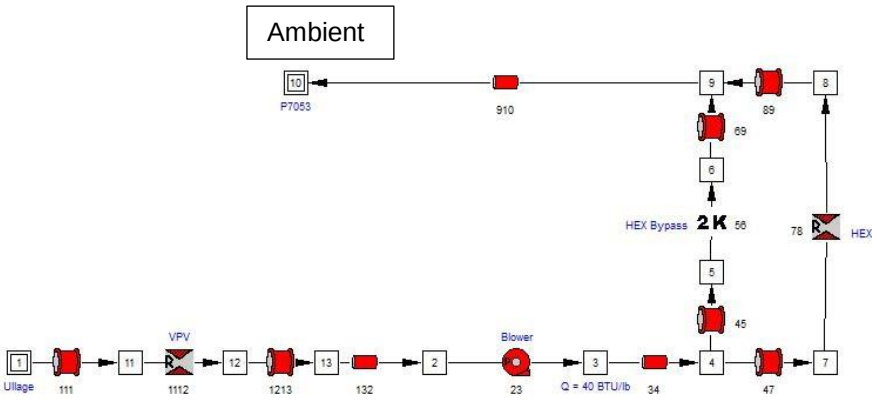

Figure 9. Unsteady Model of IVF Loop for Astros Test Series

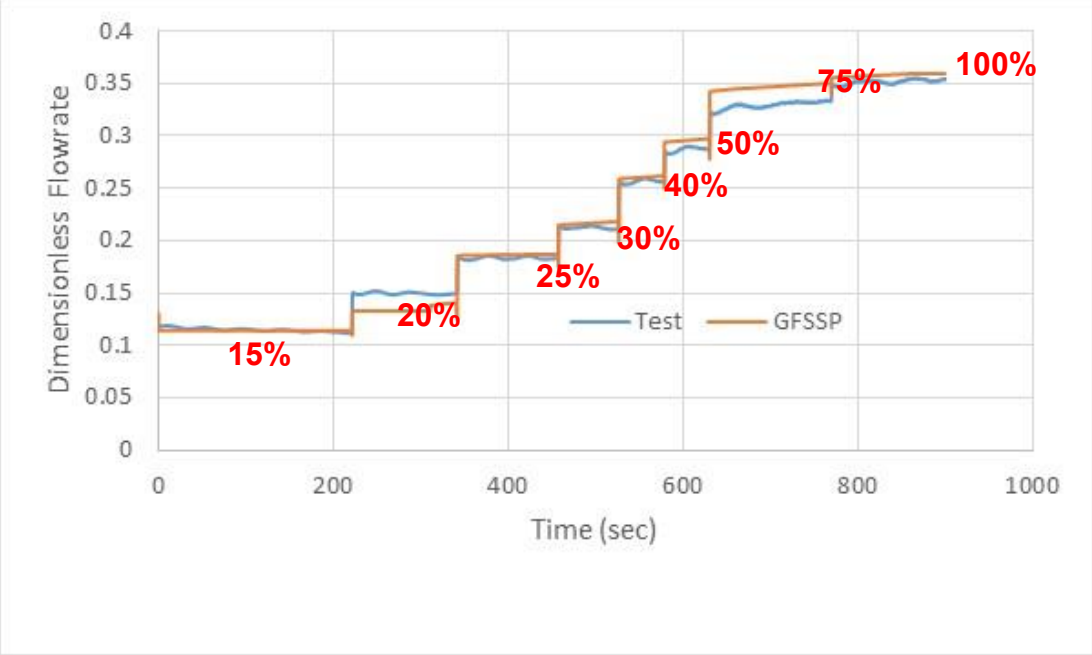

Figure 10. Comparison between predicted and measured flowrate for Astros Test

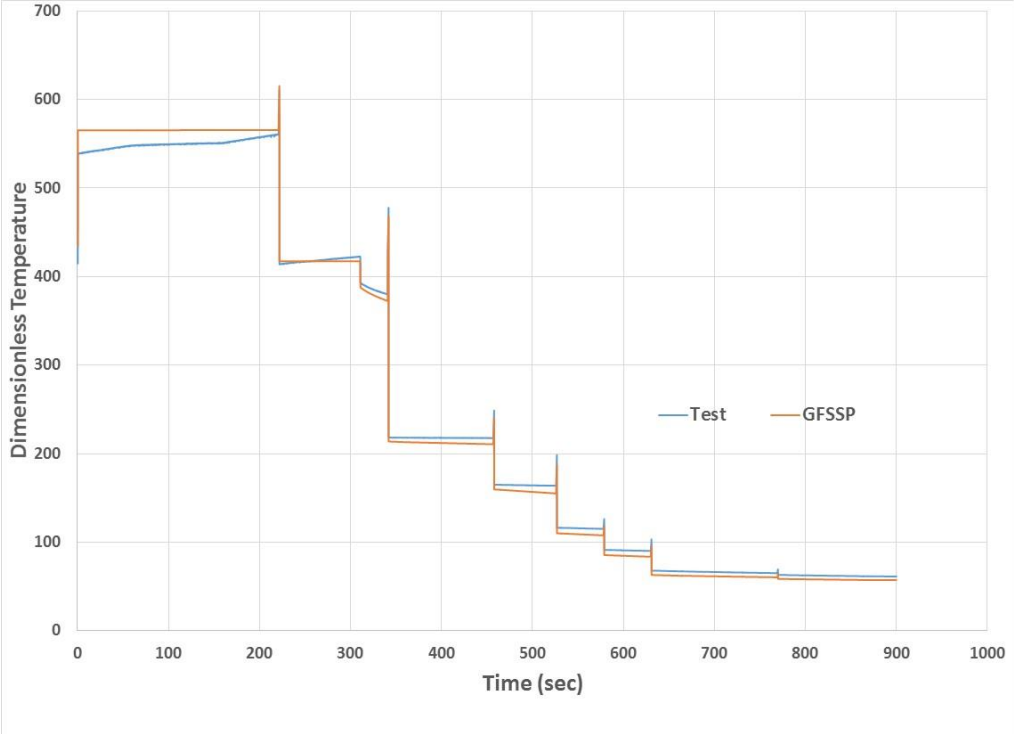

Figure 11. Comparison between predicted and measured temperature for Astros Test

Figure 10 shows the comparison of predicted and measured flowrate. The flowrate increases in steps as valve opens in steps from 15% to 100%. Figure 11 shows the dimensionless temperature history at the blower inlet as the valve opens during the test. Because temperature is normalized with dynamic head, the normalized temperature drops as valve opens. The kinetic energy of the fluid increases whereas internal energy remains more or less constant during this operation. Test results show slight increase in internal energy because of heat transfer from the ambient particularly in the beginning when flowrate was relatively low. The comparison between measurements and predictions are generally satisfactory. The observed discrepancy in flowrate and temperature is due to lack of heat transfer in GFSSP model which did not account for heat transfer from ambient to the fluid. GFSSP is predicting colder fluid which may be the cause for higher flowrate.

C. Braves Model

In the Braves test series, pressurization was a closed loop operation without any use of facility pressurant. Unlike Astros, the return leg was connected to the tank and warm gas from the IVF loop was used to pressurize the tank. The Blower motor was run at 50% power level. Separate steady-state models were developed for VPV and blower to characterize the resistance coefficient and blower efficiency to match measured pressure difference and flowrate characteristics. In this test series the heat exchanger was bypassed. With the calibrated resistance coefficient and blower efficiency, the unsteady loop model was developed and shown in Figure 12.

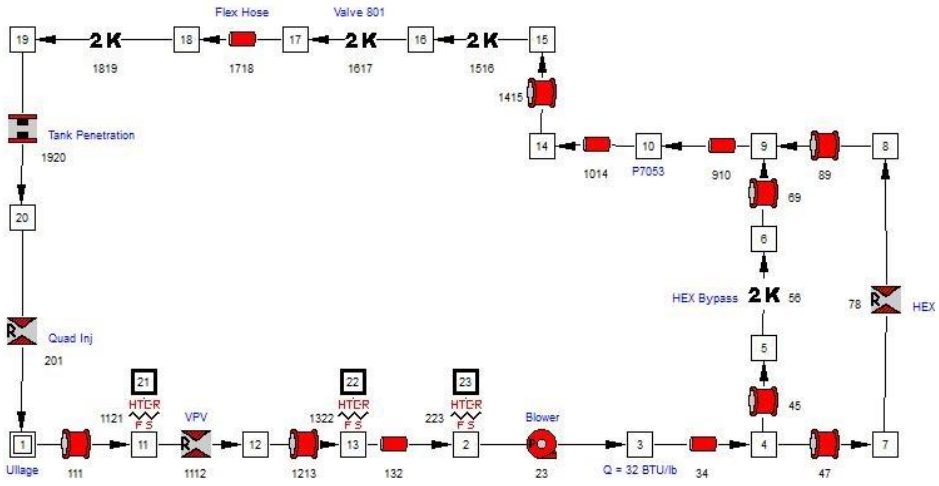

Figure 12. Unsteady Model of IVF Loop for Braves Test Series

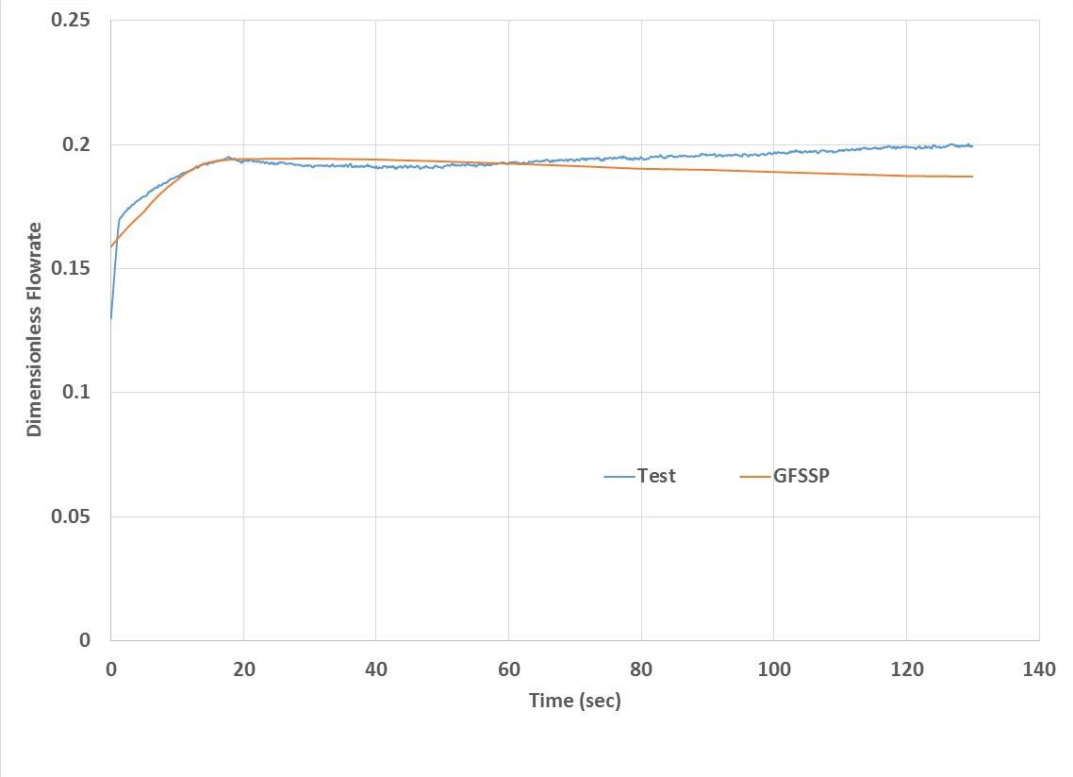

Figure 13. Comparison between predicted and measured flowrate for Braves Test

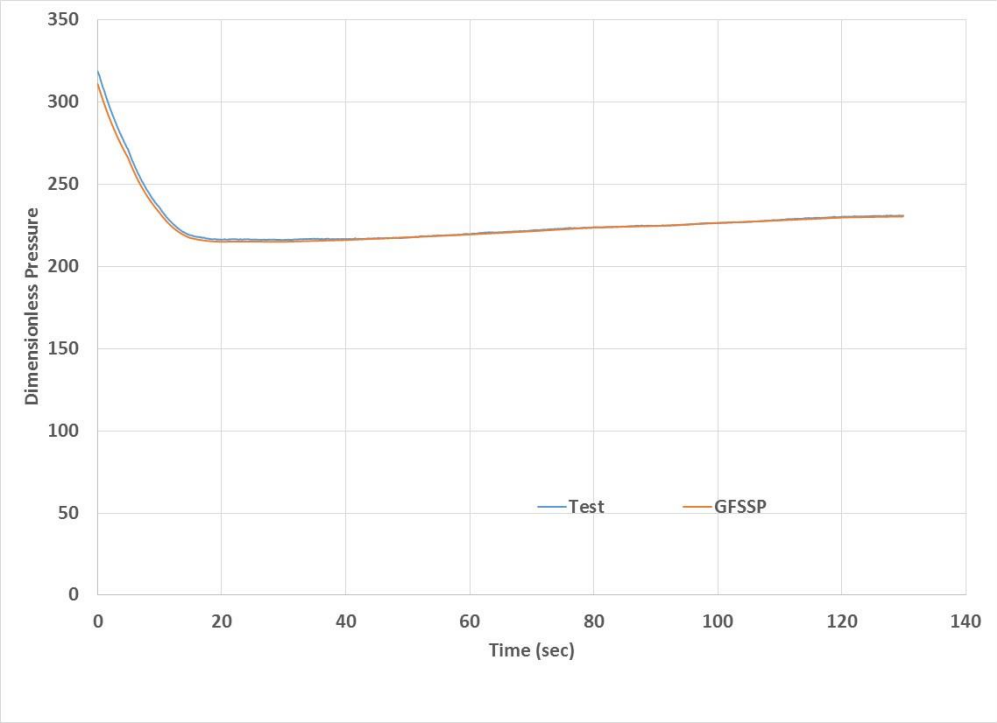

Figure 14. Comparison between predicted and measured pressure for Braves Test

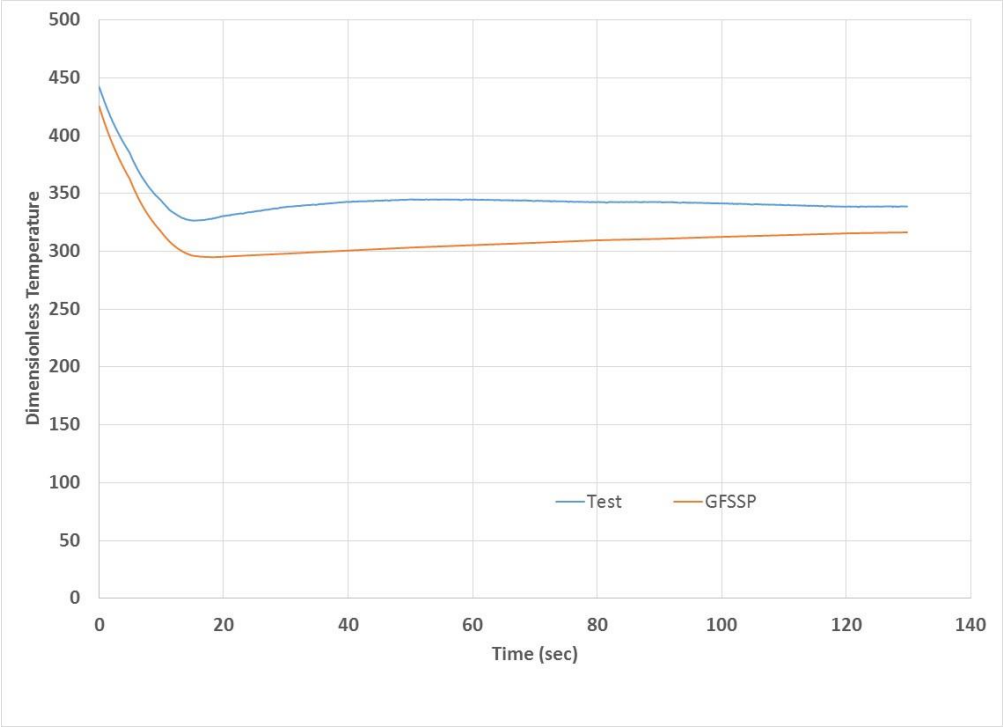

Figure 15. Comparison between predicted and measured temperature for Braves Test

In the Braves test series, the comparison between test and numerical model for flow rates and pressures and temperatures downstream of the blower are shown in Figures 13, 14 and 15 respectively. The main discrepancy is observed in temperature (Figure 15), which can be attributed to the absence of modeling heat transfer from ambient. The temperatures in the test being higher than predicted in the model are due to heat transfer from the ambient.

D. Cubs Model

In the Cubs test series, pressurization was also a closed loop operation without any use of facility pressurant. The Heat Exchanger was made active by closing the bypass. The VPV was 100% open and the blower motor was at 50% power level.

In the Cubs test series, the HEX was included. The heat exchanger model described Section IV A was integrated with the IVF loop model. A new modeling approach described in Reference 2 was adopted for integrating two models. In this approach, the IVF loop model and heat exchanger models were run separately, but the models exchanged data to provide boundary conditions for each other. This is an example of non-linear boundary conditions that change with iterations. Therefore, an iterative numerical algorithm is necessary to ensure boundary conditions are converged before the solution proceeds to the next time step. The schematic of the integrated model of the IVF loop and heat exchanger is shown in Figure 16.

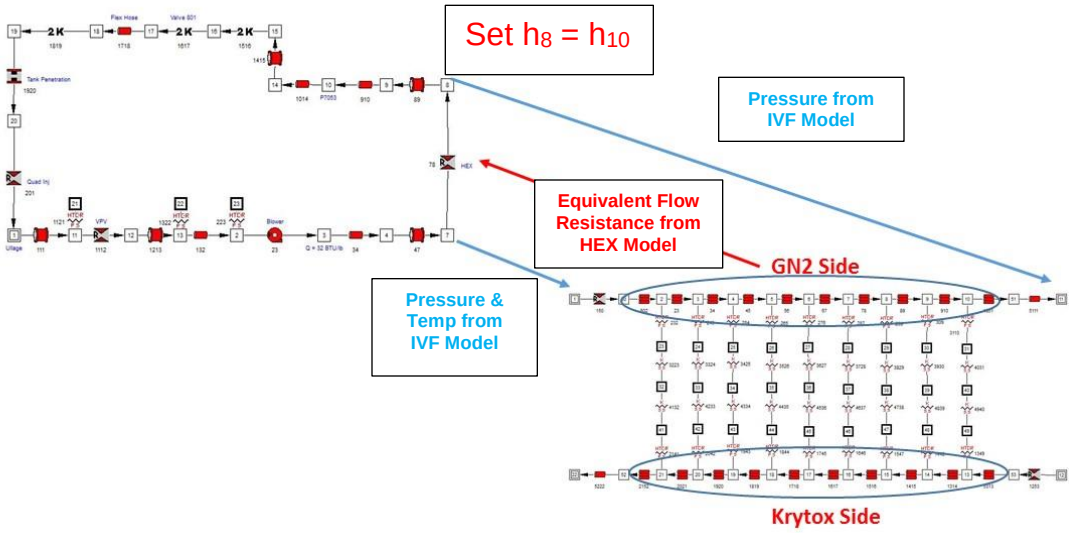

Figure 16. Unsteady Integrated Model of IVF Loop for Cubs Test Series

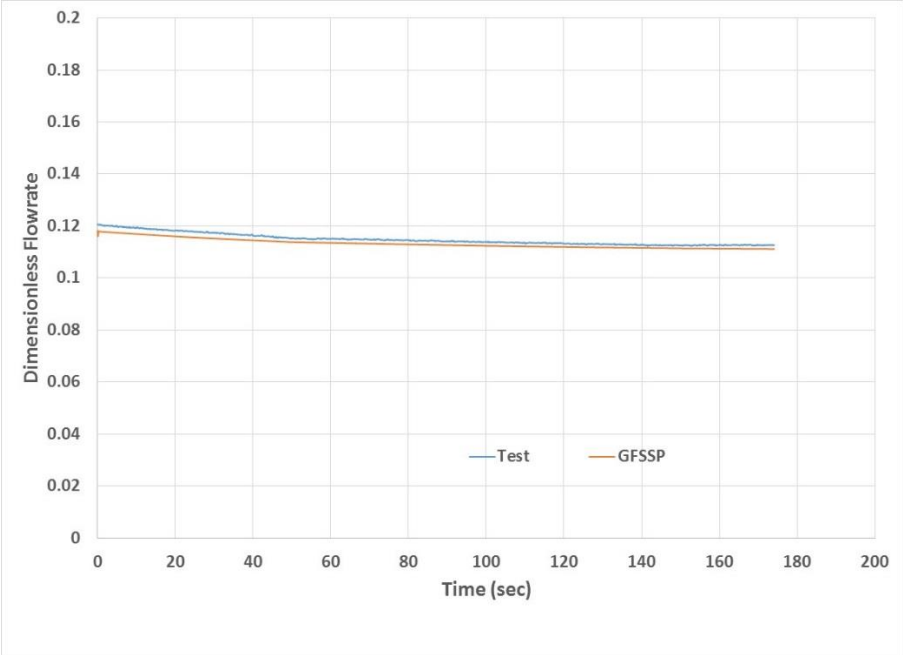

Figure 17. Comparison between predicted and measured flowrate for Cubs Test

The algorithm steps are as follows:

IVF Model

1. In the first iteration, guess resistance of Branch 78 and enthalpy at Node 8
2. Run IVF model to a converged solution with guessed values and write p_7 , T_7 and p_8 in a data file
3. Call HEX model from the User Subroutine of the IVF model

HEX Model

4. Read p_7 , T_7 and p_8 from the data file created by IVF model

5. Run the model until convergence
6. Calculate equivalent resistance of all branches in the GN2 leg of the HEX
7. Write equivalent resistance and h_{10} in a data file

IVF Model

8. Read equivalent resistance and h_{10} from the data file generated by HEX model and set $h_8 = h_{10}$
9. Check convergence of equivalent resistance and h_{10} and repeat steps 2 through 8 until convergence

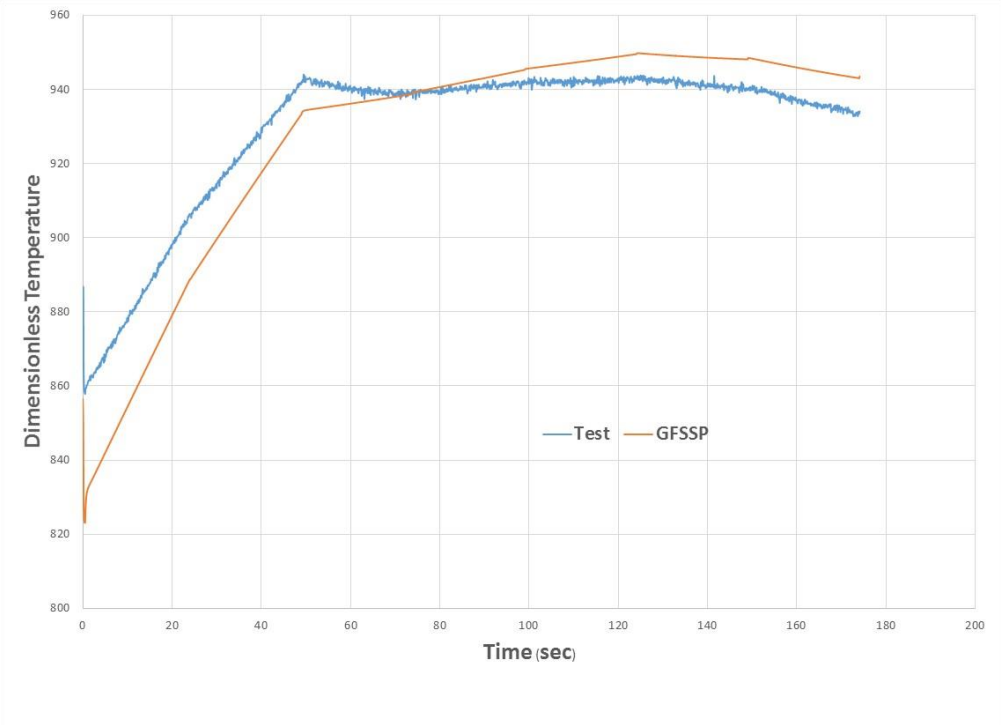

Figure 18. Comparison between predicted and measured temperature for Cubs Test

Comparison between predicted and measured flowrates and temperatures for the Cubs test series is shown in Figures 17 and 18 respectively. Excellent agreements are observed for flowrates. Discrepancies, however, are observed for temperatures that may be attributed to lack of modeling heat transfer from ambient and uncertainties in heat transfer correlation.

E. Compressor Modeling

This section describes the modeling of compressor in GFSSP. The Max Flow Test was conducted to generate a compressor map; the trend is shown in Figure 19.

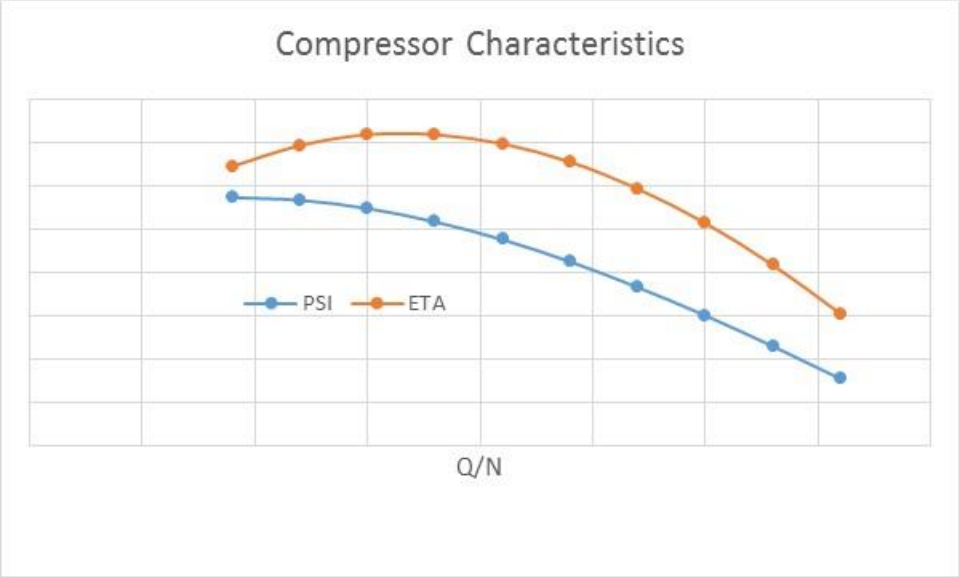

Figure 19. IVF Compressor Characteristics

The loading coefficient, PSI, expressed as g_c dH/U^2, and the isentropic efficiency ETA are plotted with Q/N where Q and N are volumetric flowrate and speed in RPM. Following are the steps to incorporate compressor characteristics in GFSSP.

1. Calculate Q

$Q = \frac{\dot{m}}{\rho}(60)$ CFM

2. Calculate Q/N

3. Obtain PSI and ETA from the characteristics

4. Calculate isentropic enthalpy rise, $\Delta h_{isentropic}$, across the compressor using the characteristic data

$$\Delta h_{isentropic} = \frac{(PSI)U^2}{Jg_c}$$

U = $\boldsymbol{\Omega}$r

$\Omega = \frac{2\pi N}{60}$

J = Conversion Constant = 778 BTU/(lb_f –ft)

5. Calculate actual enthalpy rise, Δh_{actual} , across the compressor using compressor efficiency

$\Delta h_{actual} = \Delta h_{isentropic}$ /ETA

6. Calculate pressure rise, Δp across the compressor

$\Delta p = \rho \Delta h_{actual} J$

7. Calculate Momentum Source for the compressor branch

$S_{momentum} = \Delta p\ A$; A = Branch Cross-sectional area

8. Calculate heat source due to compression

$S_{energy} = \dot{m}\ \Delta h_{actual}$

This methodology was then implemented in a flight system model using IVF as shown in Figure 20.

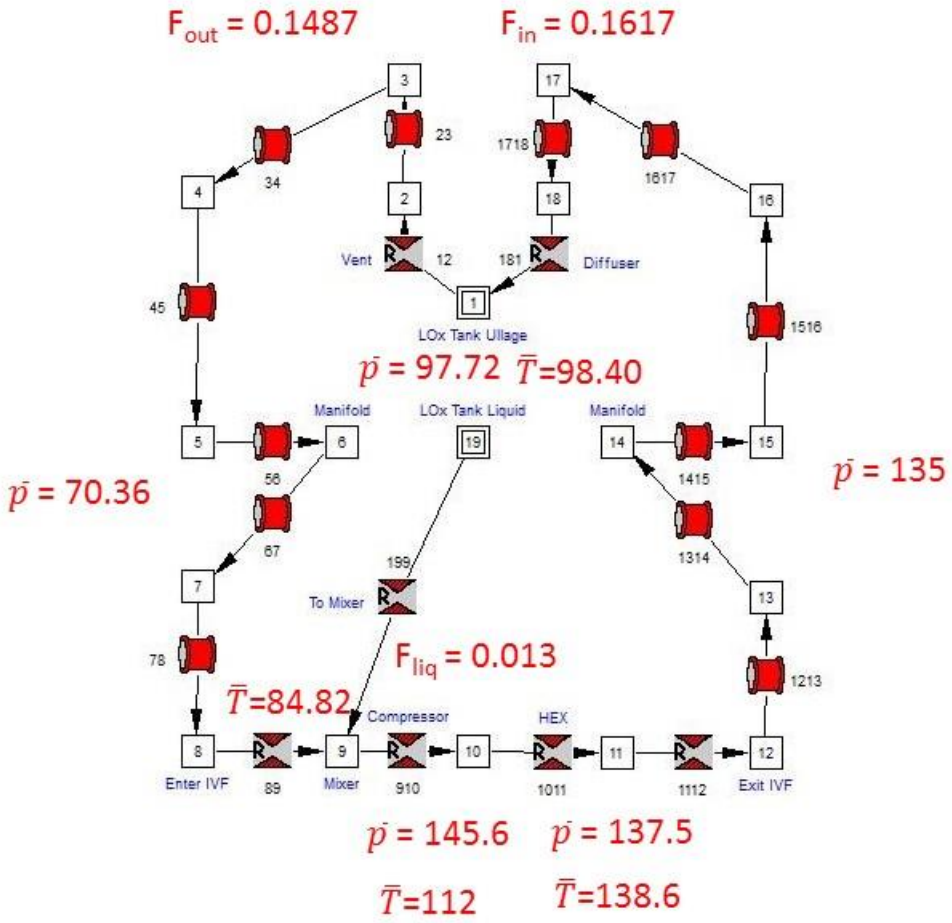

Figure 20. Sample Results of an IVF loop in a flight system

Figure 20 presents a GFSSP model of the IVF loop in a notional flight system. Boundary node 1 represents the propellant tank ullage space. Boil-off gas exits through the vent and travels through a series of pipes to enter the IVF unit. A small amount of liquid is drawn from boundary node 19 and mixed with the gas in the mixer, node 9. This allows cold gas to enter the compressor, where the pressure and temperature are raised according to the equations presented above. The temperature is then raised further in the heat exchanger. This warm gas then returns and is injected back into the tank ullage. This model is then linked with a CFD model of the ullage to provide ullage pressure and vent temperature that change with time.

III. Conclusions

This paper presents the numerical simulation of three test series designed to verify the functionality of IVF system. The test series was planned in a way to introduce new functionalities one at a time. The modeling approach was based on building several steady-state component models and verifying with test data. The component models included heat exchanger, blower, compressor, and variable position valve. The calibrated component models were then used to build the transient model of the entire IVF Loop. The transient test data for flowrate, pressure, and temperature were compared with numerical predictions. A novel method of presenting the results in a dimensionless form provided more insight to the data analysis. In general, numerical predictions compare well with test data. The observed discrepancies are mainly attributed to the lack of modeling of heat leak from ambient to the IVF Loop. A methodology has been developed to introduce compressor characteristics and tested in a flight system model with other IVF components.

IV. Acknowledgements

The authors wish to acknowledge Arthur Werkheiser of MSFC and Monica Guzik of GRC for their valuable input to this investigation and Tom Tyler of MSFC for generating the compressor map.

V. Reference

1. Frank Zegler, "An Integrated Vehicle Propulsion and Power System for Long Duration Cryogen Spaceflight" , AIAA 2011-7355, AIAA SPACE 2011 Conference & Exposition, 27-29 September 2011, Long Beach, California.
2. A.K. Majumdar, A.C. LeClair, A. Hedayat, "Numerical Modeling of Pressurization of Cryogenic Propellant Tank for Integrated Vehicle Fluid System", Paper No. AIAA 2016-4676, 52nd AIAA/SAE/ASEE Joint Propulsion Conference, Salt Lake City, Utah
3. A.K. Majumdar, A.C. LeClair, R. Moore, P.A. Schallhorn, "Generalized Fluid System Simulation Program, Version 6.0", NASA/TP—2016–218218, March 2016.